

DIACHRONIC MONITORING OF SURFACE ENERGY FLUXES BY REMOTE DETECTION IN THE NORTHERN-EST OF NIGER W NATIONAL PARK

^{1,2}Arouna Saley Hamidou, ¹Oumar Diop, and ¹Amadou Seidou Maiga.

¹ Laboratory of Electronics, Computer, Telecommunication and Renewable Energy, Department SAT, Gaston Berger University, P.O. Box 234, Saint-Louis, Senegal (French)

² Department of Physics, Faculty of Science and Technology, University of Maradi, Niger (French)

Abstract: The general objective of the present work is to contribute to a set up of an operational prototype of monitoring surface energy fluxes inside the Niger's W Park, using Landsat data and few fields' data. The model SEBAL/METRIC is used to estimate the main surface fluxes. The diachronic study of the obtained fluxes reveals constant daily mean values for a given season. During autumn 2002, the mean values of the daily evapotranspiration are almost 4mm/day. Humidity indicators are then deduced from the obtained fluxes. Their diachronic study permits to identify area with cold pixels as been less stressed than area having dry pixels. This study shows that Landsat imagery can be used, at a large scale, in monitoring the main biophysical processes occurring at the Soil-Vegetation-Atmosphere interface. Then; it allows identifying areas at risk, inside the Park, needing an adequate plan of management and conservation.

Index Terms— Energy Fluxes; Remote Detection; Soil-Vegetation-Atmosphere interface; Diachronic

I INTRODUCTION

Numerous studies were interested these last decades in the processes of transfer of mass and energy at the ground level, through estimating and diachronic studying of surface energy fluxes by remote detection. Such large-scale study is essential for a good understanding of physical processes occurring at the interface Soil-Vegetation-Atmosphere. It helps to better apprehend the combined impacts of natural variability of the climate and anthropogenic actions, observable these last decades at the global scale. Diachronic study of surface energy fluxes allows identification of degraded forest's areas or areas subject to severe hydrous stress, as shown by earlier studies [1-2]. It helps also to prevent the risk of wild forest fires, since plant's hydrous state is inversely linked to inflammability of forest resources as shown by Viegas et al. [3]. It is therefore necessary to obtain at a large scale, reliable information on land surface energy fluxes and evapotranspiration. Many methods using remote detection data in calculating surface fluxes have been in focus as shown in earlier works [4-5-6-7]. The most used

algorithms are: **SEBAL**, [8], **TSEB**, [9], **SEBI**, [10], **S-SEBI**, [5]; **SEBs**, [11] and **METRIC**, [6].

In Niger, studies using remote data have been conducted in order to improve the management of the park, as shown in earlier studies [12-13-14-15]. Still, no study on surface energy fluxes and their relationship with soil's state has yet been conducted. It is so necessary to fill this gaps. The general objective of the present work is to contribute in the development of an operational prototype of monitoring those fluxes, using many Landsat data. This prototype is based on simplified procedures, to make it easy operational and reproducible for field's managers in sahelian's conditions, where field data are rare and inaccessible.

II CHARACTERISTICS OF THE STUDY AREA

The study area is located in Niger Republic (West Africa), **Fig.1**. It lays between longitudes 2°25'E and 2°45'E and

latitudes 12°25'N et 12°40'N. It covers a surface area of 63.000 ha. It is composed of a protected area in the south, inside the Park, and a non protected area in the North, outside the park. The two areas are separated by a natural border, the Niger River.

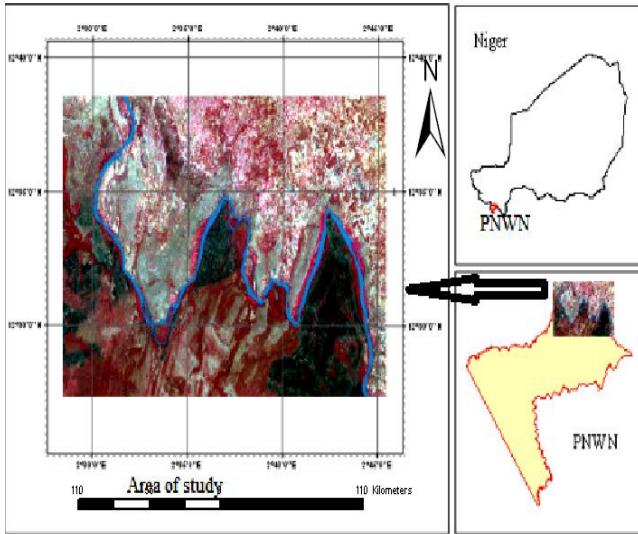


Fig 1. Geographic position of the study's area

It is a tropical type with soudano-sahelian climatic system. Four types of geomorphologies are identified and mapped in the area: rocky plateaux, pediments and drains, battleships plateaux and the intermediary forms as shown by Benoit, [13].

III MATERIALS AND METHODS

The data used in this study are from six Landsat TM and ETM+ detectors, path 192 row 051, acquired during autumn in Niger, with almost clear sky conditions where, one can minimise the effects of cloud on the reflectance detected by the satellite.

Solar conditions, on the day of acquisition of each image are calculated in this study. The obtained values and the dates of acquisition are presented in **Table 1**. They are used during atmospheric corrections of the reflectance detected by the satellite (using MODTRAN 4/FLAASH model according to Hoke, [16]) and during correction of the effects of relief on the reflectance (using a Digital Elevation Model of the study's area). They are also used during the parameterisation of the surface energy balance equation, given as:

$$RN + H + G + LE = 0 \quad (1)$$

Where, RN ($W m^{-2}$): net incident solar radiation flux; H ($W m^{-2}$): sensible heat flux; G ($W m^{-2}$): soil heat flux; LE ($W m^{-2}$): latent heat flux.

The raw Landsat images, used in this study, are of level 1 delivered by USGS, (UTM, and WGS 84 Zone 31). The

pixel size is 30m x 30m. The supervised classification, by maximum likelihood method, is applied to classify each image. The use of this method is motivated by our well-known knowledge of the study's area and because through experience, supervised classification becomes easier and more correct. Then, the six images were classified using this method. The results of this classification, for image acquired on 1st February 1990, are presented in **Fig. 2**.

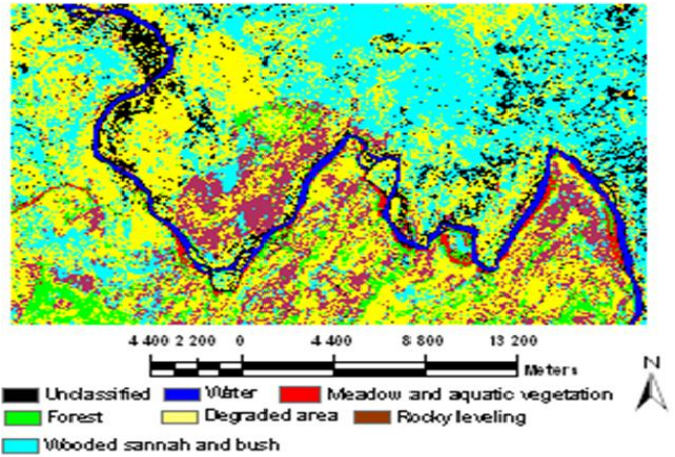


Fig 2. Land use/occupation on 1st February 1990

The maps of this classification are indispensable at the time of executing SEBAL/ Metric, precisely while choosing the dry and cold pixels. These pixels (called anchor pixels) are pixels on which thermal gradient, dT and sensible heat fluxes, H are calculated. Luminances of optic domains (Visible, near and mean infrared) were converted into reflectances before mapping the surface energy fluxes. The obtained reflectances are then used to calculate the following inputs parameters: surface Albedo (α), Index of Vegetation (NDVI) and Surface Temperature (TS). The theoretical basis of mapping evapotranspiration from remote detection data are nowadays well documented [17-5-6]. Steps given by Allen *et al*, [6] were used in this study to map the surface energy fluxes and evapotranspiration. The basic Eq. (1) had been that of surface energy balance. Thus, the equivalent energy of evapotranspiration, LE has been estimated as a residual of Eq. (1), applied to each pixel. It is calculated according to:

$$LE = RN - H - G \quad (2)$$

Where, RN is given by:

$$RN = (1 - \alpha) R_{global} + R_{atm} \downarrow - R_{suf} \uparrow \quad (3)$$

With, R_{global} : The incident global solar radiation, (W/m^2) partially reflected by the surface in function of surface albedo, $R_{atm} \downarrow$: The incident atmospheric longwave radiation, (W/m^2) and $R_{suf} \uparrow$: Shortwave radiation emitted by earth's surface, (W/m^2).

H is the sensible heat flux, (W/m²) obtained by an iterative approach, from the aerodynamic equation, given by:

$$H = (\rho_{\text{air}} C_p dT) / r_{\text{ah}} \quad (4)$$

With: ρ_{air} = air density in Kg m⁻³; $C_p = 1004 \text{ J Kg}^{-1}\text{K}^{-1}$ (specific capacity of air); dT (°K) = Thermal gradient of air (between $Z_1 = 0.1 \text{ m}$ and $Z_2 = 2 \text{ m}$ above the ground),

r_{ah} = aerodynamic resistance to heat transfer in s m⁻¹, between two nearest surfaces, separated by distance $Z_2 - Z_1$.

G (W/m²) is the soil conduction flux calculated according to Bastiaanssen, [17]:

$$G = [(TS - 273.16) (0.0038 + 0.0074\alpha) (1 - 0.98\text{NDVI})] / \text{RN} \quad (5)$$

In Eq. (3) the surface albedo α is calculated according to Liang *et al.*:

$$\alpha = 0.356r_1 + 0.13r_3 + 0.373r_4 + 0.085r_5 + 0.072r_7 - 0.0018 \quad (6)$$

Where the r_i is the reflectance in channels i (1; 3; 4; 5 et 7) of Landsat satellite, corrected from atmospheric and relief effects. These reflectances are deduced from the corresponding luminance $L_{\lambda i}$. The global solar radiance or incoming shortwave radiation is calculated using formula:

$$R_{\text{global}} = (G_{\text{cs}} \times \cos\theta \cdot \text{img} \times \tau_{\text{sw}}) / d^2 \quad (7)$$

With, $G_{\text{cs}} = 1367 \text{ W m}^{-2}$ (solar constant), $\cos\theta \cdot \text{img}$ (Integrate the solar declination; the latitude; the slope; the surface aspect angle and solar hour angle of our study area) is the spatial distribution of solar declination angle, d = relative mean distance between the earth and the sun; τ_{sw} = transmissivity of the atmosphere, calculated in function of air effective emissivity.

The atmospheric radiation $R_{\text{atm}} \downarrow$ is calculated according to the Stefan-Boltzmann's formula:

$$R_{\text{atm}} \downarrow = \epsilon_s \epsilon_a \sigma T_a^4 \quad (8)$$

With, ϵ_s : The surface emissivity (it corresponds to the conversion factor of thermodynamic energy to radiative energy), expressed in function of NDVI.

ϵ_a : Air effective emissivity; σ : Boltzmann's constant. The radiation emitted by the earth surface $R_{\text{suf}} \uparrow$ is calculated according to Stefan-Boltzmann's formula:

$$R_{\text{suf}} \uparrow = \epsilon_s \sigma T_s^4 \quad (9)$$

With T_s calculated from the radiative surface temperature T_{RS} ($T_s = (T_{\text{RS}} / \epsilon_s)^4$ i.e. by simple inversion of Stefan-Boltzmann's Law). T_{RS} is given by the following formula:

$$T_{\text{RS}} = K_2 / \ln [(K_1 / r_{\text{c}(6)} + 1)] \quad (10)$$

K_1 and K_2 are specific constants of calibration for each type of Landsat satellite. The values of the constants are given inside the header files of each image, downloadable at the same time with the image. $r_{\text{c}(6)}$ is the real radiance emitted by the surface, corrected from the atmospheric and relief effects.

Calculation of H from formula (4) requires simultaneous existence of dry pixels and cold pixels on the site of study as shown by Allen *et al.*, [6]. The supervised classification has permitted the identification of such pixels: dry pixels are rocky levelling and burned area and cold pixels are meadow and aquatic vegetation.

To spatialize dT , we have first determined the values of H on dry pixels (H_{dry}) and after on cold pixels (H_{cold}). They obtained values are then used to estimate the thermal gradient dT using an iterative process, starting by applying neutral stability conditions of the atmosphere, until obtainment of dT convergence after successive corrections of the atmospheric stability, precisely on the aerodynamic resistance. The mapping of dT is made possible by assuming a linear relation with T_s , according to Allen *et al.*, [6]:

$$dT = a - b T_s \quad (11)$$

Where b and a , constants estimated on anchor pixels (dry/cold pixels), chosen on each image.

The spatial distribution of dT is used in another iteration process from Eq. (4), thus allowing the mapping of H. The spatial distribution of the other instantaneous fluxes allows mapping the latent heat flux, H and then the instantaneous evapotranspiration ET_{inst} which is calculated according to the following equation:

$$ETR_{\text{day}} = FE * R_{\text{n day}} \quad (12)$$

Where, FE (in French) is the Fraction of Evaporation considered constant for a given day, as suggested by Bastiaanssen *et al.*, [4]:

$$FE = LE_{\text{inst}} / (R_n - G) \quad (13)$$

LE_{inst} is the instantaneous latent heat (LE_{inst}) and $(R_n - G)$ is the available energy at earth's surface.

$R_{\text{n day}}$ is the net daily radiation given by:

$$R_{\text{n day}} = (1 - \alpha_0) * R_{\text{g day}} - 110 * \tau_{\text{day}} \quad (14)$$

R_{gday}: is the global daily radiation and τ_{jour}: daily transmissivity of atmosphere (expressed as function of sunstroke fraction n/N) given by:

$$\tau_{day} = 0.25 + 0.50 * n/N \quad (15)$$

R_{gday} is esteemed from the daily exo-atmospheric radiation K_{exo} and τ_{day}:

$$R_{gday} = K_{exo} * \tau_{day} \quad (16)$$

Known that, to evaporate 1Kg of water we need 2, 45*10⁶ joules (latent heat of evaporation), we have ETR_{day} in mm day⁻¹calculated as:

$$ETR_{day} = ETR \text{ (joule)} / (2, 45 * 10^6) \quad (17)$$

IV Results and discussion

A. spatial and diachronic analyses of the inputs parameters and the obtained fluxes

The inputs parameters of the model, i.e. surface temperature, surface Albedo and NDVI are estimated, in space at pixel scale and in time at the different dates of acquisition, **Table1**. This table and the figures of **appendis A**, (Fig1A, Fig2A, and Fig3A) show a very spatial variability of these inputs. This variability can be explained by the heterogeneous character of the study's area, observable in **Fig.2**. From **Table1** we can observe that when the NDVI is high the corresponding temperature is low, vice versa. This result is general; a ground which vegetal cover increases sees its surface temperature decreasing. This could be due to the fact that the vegetation reduces the aerodynamic resistance of the evapotranspiration. A complementary study is necessary to be conducted in order to verify such hypothesis.

Table 1: Values of the inputs for each day of image acquisitions

acquisition date	TS (°K)			Albedo			NDVI		
	Min	Moy.	Max	Min	Moy.	Max	Min	Moy.	Max
01/02/1990	294.27	313.14	320.69	0.04	0.24	0.51	-1.03	0.16	0.37
04/10/1992	298.83	307.11	315.13	0.10	0.20	0.34	-0.27	0.28	0.67
30/11/1998	294.15	308.95	319.83	0.05	0.18	0.40	-0.53	0.16	0.72
02/02/2002	290.98	307.31	314.34	0.10	0.23	0.35	-0.28	0.26	0.52
17/11/2002	296.93	313.82	328.75	0.05	0.19	0.42	-0.40	0.14	0.70
05/02/2003	294.48	313.12	322.09	0.06	0.21	0.34	-0.67	0.16	0.78

Surface temperature is among the most key parameters that control the whole physical processes occurring at Sol-Vegetation-Atmosphere interface. It is therefore important to get more reliable information on this parameter. Thus, its distributions (spatial and temporal) were analysed. The spatial distribution shows that the surface temperature varies between 296.93°K and 328.75°K, **Fig1A**, with a mean value of 313.82°K. These values are in the same order of magnitude as the ones obtained by remote detection in areas with almost the same type of climate as our study's area, [20-21]. Minimum values correspond to cold pixels (water, meadow and aquatic vegetation) and high values to hot pixels (rocky levelling and burned area). The evolutions of surface temperature, in terms of vegetation abundance (through the vegetation index, NDVI) were also analysed. On 4th October 1992, where the vegetation is abundant (mean NDVI =0.28, with maxima reaching up to 0.67) lowest surface temperature is obtained (TS = 307.11°K). This could be due to the fact that vegetation reduces the resistance of surface evapotranspiration, this induced diminish of surface temperature.

The temporal comparison between the mean daily values of the evapotranspiration, on the following days: 04/10/1992, 30/11/1998, 02/02/2002, and 17/11/2002, shows that these values are practically constant (4mm/day), as shown in **Table 2**. Indeed, except precipitations and wind all the others biophysical parameters are generally constant for a given season, like in autumn, season during which the study's images were acquired. On the other hand, values of the remaining fluxes i.e. the sensible heat flux, H and the conduction flux G, are varying both in space, figures of **appendis B** (Fig1B, Fig2B, Fig3B) and time, **Table2**, due to the variability of the phenomenon of convection.

Table 2: Values of surface energy fluxes and evapotranspiration

Acquisition date	G (W m ⁻²)			H (W m ⁻²)			ETR _{day} (mm day ⁻¹)		
	Min	Moy	Max	Min	Moy	Max	Min	Moy	Max
01/02/1990	0.35	5.97	64.20	0.003	12.48	21.52	0.027	1.33	5.27
04/10/1992	69.87	118.82	193.76	0.003	65.32	459.88	0.073	4.47	8.09
30/11/1998	10.18	54.20	131.65	0.003	67.08	111.95	0	4.18	7.07
02/02/2002	24.11	58.32	72.40	0.003	185.21	347.01	1.55	4.28	7.42
17/11/2002	0.07	17.42	70.29	0.003	349.86	170.75	0.40	3.13	7.12
05/02/2003	0.29	26.01	74.41	0.003	139.37	71.57	0	1.48	7.26

B. characterizations on the soil’s state

Before characterizing the soil’s state, the diagrams defined by the relation between TS and NDVI were used to locate the dry/cold pixels, using the triangle’s method, [2-19]. The relation between TS and albedo was then used to confirm the positions of such pixels. For the image, acquired on 5th February 2003, a threshold albedo of 0.2905 was obtained for corresponding TS of 313.6°K, **fig.3**.

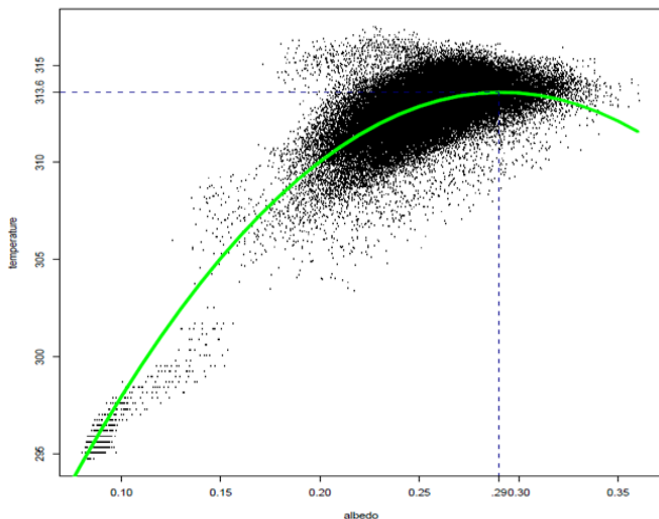


Fig 3. Surface temperature function of Albedo

Cold pixels are pixels having cold temperatures with albedo lesser than threshold albedo. Dry pixels are pixels having high temperatures with albedo greater than threshold albedo. After locating the dry/cold pixels we have analyzed the spatial and temporal variability of the surface energy fluxes of two different areas extracted from the same image, those areas are named **A** and **B**: **A** has more cold pixels (well-watered and fully vegetated) than **B** and **B** has more dry pixels (almost bare soil not too much covered). Mean values of humidity indicators over area **A**, **Table3a**, shows highest values of evaporation fraction and daily evapotranspiration. On the other hand, these values are lowest over **B**, **Table3b**. This is explained by the fact that an increase of albedo induces diminish of energy absorbed by the surface and thus, lesser temperature; as regulation by latent heat flux is no more possible. Covered surfaces have the highest values of fraction of evaporation. This has grave consequences, expressed as diminish of soil humidity and drainage of vegetation, more marked in case of lack of water. During the months of February 1990 and 2003, humidity indicators of zone **B** have the lowest mean values compared to those of zone **A**, **Tables3a and 3b**. Hydrous stress is thus more marked over zone **B**. According to Thiery and al. [22], it was during the last 90’s and 2000’s decades that negatives impacts of climate changes are observed in sahelian’s regions. It is therefore highly probable that these observed

lowest values are linked with the impacts of climate changes.

Table 3a and 3b: Mean daily values of humidity indicators on zone A and on zone B

Table 3a: Zone A

Acquisition date	LE (W m ⁻²)	TS (°K)	FE	ETRday (mm/ day)
01/02/1990	54.90	308.47	0.73	3.27
04/10/1992	594.74	303.16	0.98	8.60
30/11/1998	319.31	304.10	0.97	6.23
02/02/2002	477.67	303.89	0.84	5.73
17/11/2002	342.55	306.78	0.78	4.97
05/02/2003	88.37	310.55	0.51	3.42

Table 3b : Zone B

Acquisition date	LE (W m ⁻²)	TS (°K)	FE	ETRday (mm/ day)
01/02/1990	3.81	312.94	0.15	0.66
04/10/1992	493.15	307.00	0.95	6.66
30/11/1998	172.73	307.93	0.77	4.52
02/02/2002	317.98	307.44	0.64	3.99
17/11/2002	174.07	313.76	0.48	4.97
05/02/2003	14.81	312.56	0.15	0.91

V CONCLUSION

This study has permitted a diachronic monitoring of the main surface energy fluxes and humidity indicators. Obtained maps have reflected the dynamic of the study’s area, for different inputs of the model used. The same dynamic was observed for the main resulting fluxes i.e. flux of conduction, sensible heat flux and latent heat flux. The monitoring has allowed also the characterization of the soil’s state and identification of areas that can be subject to severe hydrous stress. By lack of sufficient and pertinent field’s data we are not able to verify some hypothesis we made in this study. More images and field’s data are necessary to get

interpolated daily, monthly and seasonal values. But the obtained values are in the same order of magnitude as those encountered in the literature for regions having almost the same type of climatic characteristics as our study's area. We are planning to conduct a campaign of field's data collecting and a real time satellite image downloading, over a long period, through an important research project, in collaboration with some partners. It will contribute in setting up the operational prototype of monitoring surface energy fluxes inside the Park. This will help to better apprehend, inside the Park, the various biophysical processes occurring at the soil-Vegetation- Atmosphere interface. Then; it allows identifying areas at risk, needing an adequate plan of management and conservation.

VI RECOMMANDATIONS

As shown through this study, remote sensing can be a powerful mean of studying surface energy fluxes at a large scale. New generations of Satellites with a temporal resolution of 3 days, like Formosat and Venus, offer the possibilities to utilize the same approaches developed in this study. Many field data are also necessary to validate the obtained surface energy fluxes by remote sensing. Then, to conduct a better diachronic monitoring of surface energy fluxes, at a large scale, we highly recommend conducting the following field's works:

1. To realize a big campagne of field's data collection, at pixel scale and at real time, corresponding to the passage of the satellite over the pixel;
2. To realize and test an operational prototype of continuous mapping of surface energy fluxes, using satellite's informations;
3. To develop algorithms permitting the interpolation of the surface energy fluxes at the day's basis, seasonal's basis and annual's basis, between many dates of image's acquisition.

Taking in account the above three aspects in the monitoring processes is the only necessary condition for a better utilization of obtained surface energy fluxes in the hydrologicals and environmental's thematic.

VII ACKNOWLEDGMENT

The authors wish to thank Pr. Saadou Mahamane and Pr. Ali Mahamane, respectively rector and vice rector of the University of Maradi, for their helpful contributions. This work was supported in part by the budget of the University of Maradi.

REFERENCES

[1] Hamimed A., Mederbal K., Khaldi A. " Utilisation des données satellitaires TM de Landsat pour le suivi de

l'état hydrique d'un couvert végétal dans les conditions semi-arides en Algérie". *Télétection* 2: 29-38, 2001.

[2] Mehor. M, Hamimed. A, Khaldi. A, Seddini.A, Abdeslam. B. "Spatialisation de la température et des flux énergétiques de surface à partir des données satellitaires Landsat ETM+". *Revue Française de photogrammétrie et de télédétection*, N°190, pp.15-17, 2008

[3] Viegas D.X., Viegas T.P., Ferreira A.A.D. "Moisture content of fine forest fuels and fire occurrence in Portugal". *The International Journal of Wild land Fire*, vol. 2 (2): 69-85, 1992.

[4] Bastiaanssen, W.G.M., M. Menenti, R.A. Feddes and A.A.M. Holtslag. "Remote sensing Surface Energy Balance Algorithm for Land (SEBAL): 1. Formulation". *J. Hydrol.*, 212-213: 198-212, 1998.

[5] Roerink, G.J., Z. Su and M. Menenti. S-SEBI. "A simple remote sensing algorithm to estimate the surface energy balance". *Phys. Chem. Earth*, 2000

[6] Allen, R.G., T. Masahiro and T. Ricardo. "Satellite-based energy balance for mapping Evapotranspiration with internalised calibration (METRIC)-Model". *J. Irrigat. Drain. Eng.*, 133(4): 395-406, 2007.

[7] Hamimed, A., Z. Souidi and K. Mederbal. "Spatial évapotranspiration and surface energy fluxes from Landsat ETM + data: Application to a mountain forest region in 2009 Algeria". *JAS AUF Alger*, November, 2009.

[8] Bastiaanssen, W.G.M. "Regionalization of surface fluxes densities and moisture indicators in composite terrain". Ph.D. Thesis, Agricultural University Wageningen, 273 p, 1995.

[9] Norman, J.M., Kustas, W.P. and Humes, K.S. "Source approach for estimating soil and vegetation energy fluxes in observations of directional radiometric surface temperature". *Agricultural and Forest Meteorology*, 77:263-293, 1995.

[10] Menenti, M.; Choudhury. "Parameterization of land surface evaporation by means of location dependent potential evaporation and surface temperature range". *Proceedings of IAHS conference on Land Surface Processes*, 1993.

[11] Su, Z. "The Surface Energy Balance System (SEBS) for estimation of turbulent heat fluxes at scales ranging from a point to a continent". *Hydrol. Earth Syst. Sci.*, 6(1): 85-99, 2002.

[12] Couteron, P. "Reflection on spatial models for land Sudano-Sahelian area. DEA memory structures and spatial dynamics". University of Avignon, pp: 61, 1992.

[13] Benoit, M. "Status and use of land on the outskirts of the National Park of "W" in Niger. Contribution to the study of natural and plant resources Tamou's Township Park and the "W". Office of Scientific and Technical Research Overseas (ORSTOM) Niamey, Niger (In French), 1998.

[14] Inoussa, M.M., A. Mahamane, C. Mbow, M. Saadou and B. Yvonne. "Spatio-temporal dynamics of wood-

- land in the W National Park of Niger (West Africa) ". Drought, 2011.
- [15] Diouf. A. "Influence des régimes des feux d'aménagement sur la structure ligneuse des savanes Nord-soudaniennes dans le Parc du W (Sud Ouest NIGER)". Thèse de doctorat, soutenue en 2013 à l'école inter facultaire de bios ingénieurs de l'Université Libre de Bruxelles, 2013.
- [16] Hoke.T. "MODTRAN4. Radiative transfer modelling for atmospheric correction". Proceeding of the Optical Spectroscopic Techniques and Instrumentation for Atmospheric and Space Research III, SPIE July 1999.
- [17] Bastiaanssen, W. "SEBAL-based sensible and latent heat fluxes in the irrigated Gediz Basin, Turkey". J. Hydrol., 229(1-2): 87-100, 2000.
- [18] Liang, S., C.R. Shuey and C. Daughtry. "Narrowband to broad band conversions of land surface Albedo: II validation". Remote Sensing Env. 84: 25-41. Penuelas, 1993. The reflectance at 950-970 mm regions as an indicator of water status". Int. J. Remote Sensing, 14: 1887-1905, 2002.
- [19] Arouna, S.H., Oumar.D, Amadou.S.M. "A Spatial Analysis of Surface Energy Fluxes and evapotranspiration in the Northern-east of Niger W National Park". Research Journal of Environmental and Earth Science 5(3): 123-130, 2013 ISSN: 2041-0484; e-ISSN: 2041-0492 © Maxwell Scientific Organization, 2013.
- [20] Bashir, M.A., Takeshi, H., Haruya,T., Abdelhadib, A. W., Akio, T. "The spatial analysis of surface temperature and evapotranspiration for some land use/cover types in the Gezira area, Sudan". Research project supported by the grants-in-aid (No.16405031), from the Japan Society for the promotion of Science, 2007.
- [21] Penuelas, C. "The reflectance at 950-970 mm regions as an indicator of water status". Int. J. Remote Sensing, 14: 1887-1905, 1993.
- [22] Thierry, M., Erwann, F., Joan, B. "Evaluation des risques liés aux variations Spatiotemporelles de la pluviométrie au Sahel", 2007.

ABBREVIATIONS LIST

- ETR_{day}**: daily evapotranspiration.
- ETM+**: Enhanced Thematic Mapper plus.
- NDVI**: Normalized Difference Vegetation Index.
- PNWN**: Parc National du W du Niger (French).
- METRIC**: Mapping evapotranspiration with high Resolution and Internalized Calibration.
- SEBAL**: Surface Energy Balance Algorithm for Land.
- SEBI**: Surface Energy Balance Index.
- S-SEBI**: Soil Surface Energy Balance Index
- SEBs**: Soil Energy Balance System.
- TM**: Thematic Mapper.
- TSEB**: Two-Source Energy Balance algorithm.